Acyclic Poset Multiplihedra and their Quotients

Stefan Forcey[*] Ross Glew[†]
Chris Tapo[*]

sforcey@uakron.edu r.glew@herts.ac.uk cet64@uakron.edu

21st July 2026

Abstract

Two families of polytopes underlie the combinatorics of associative operations. Associahedra and multiplihedra respectively capture the information in the operation itself and in the morphisms that respect that operation. The first applications of these polytopes, from Stasheff, were for modeling homotopy associative spaces and their homotopy homomorphisms. Later, lax and weak higher categories used both as the shapes of commuting diagrams. More recently, the associahedra have been generalized to versions based on graphs, and then to posets: the acyclonestohedra. Here we use the graph multiplihedra to define and realize new multiplihedra for the acyclonestohedra. Quotients of these are also studied, concluding with the interval polytopes of the order polytopes of posets.

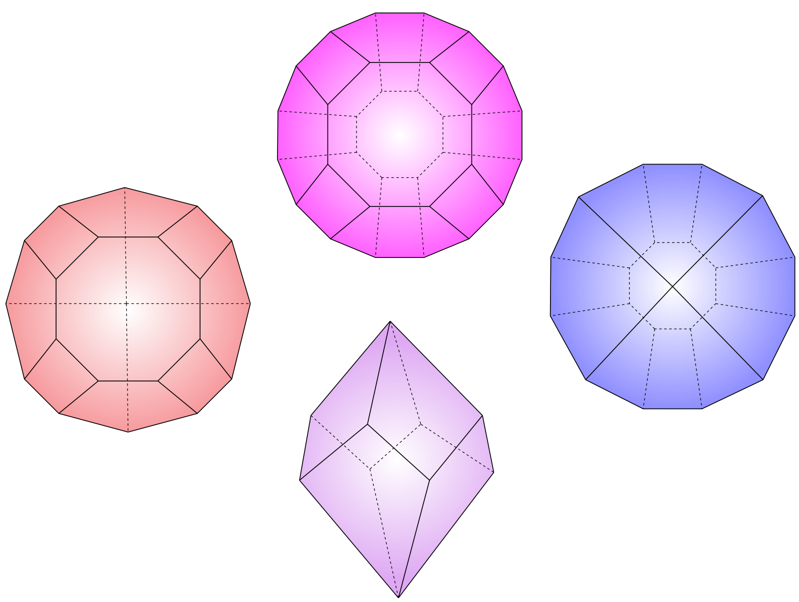

Figure 1: Cast of characters: the acyclic multiplihedron and its quotients for the bowtie poset.

[*]Department of Mathematics, University of Akron, Akron, Ohio 44325, United States of America
[†]Department of Mathematics and Theoretical Physics, University of Hertfordshire, Hatfield, Hertfordshire AL10 9AB, United Kingdom

Contents

1 Introduction and Summary

Tubings, nestings, and pipings are special subsets of a power set $\mathcal{P}(S)$ of a given *ground* set S. The definitions of each begin with the elements of the power set they may contain: the *tubes, nests, or pipes*. Often that initial collection of subsets $\mathcal{B} \subseteq \mathcal{P}(S)$ is called a *building* set. The axioms for a building set $\mathcal{B}$ are: 1) the empty set is not a member of $\mathcal{B}$; 2) the building set $\mathcal{B}$ must include all the singletons of S; and 3) for any two elements of $\mathcal{B}$, if they have nonempty intersection, then their union is also in $\mathcal{B}$. In this paper we will deal with tubes of a graph as defined in [10], which comprise a building set on the nodes of that graph. Pipes as defined in [17] are special subposets of elements of a poset. Pipes do not make up a building set of the poset elements; but instead they are a special class of tubes of the line graph of the Hasse diagram of the poset. The term nest is used in [19] for what turn out to be pipes, but for a poset that has a Hasse diagram that is a tree, or forest. Historically then tubes of a graph were defined first, then nests and pipes of a poset were described independently, then nests were realized to be a specialization of pipes, specifically in [12], and finally, it was pointed out in [20] and [21] that pipes are secretly special versions of graph tubes.

We will go over the definitions in the next section. But since all three sorts of subset are in the class of tubes of a graph, we will often call them tubes for ease of the discussion, leaving to the context what special sort of tube they are. Thus a tubing, nesting, or piping is a collection of tubes obeying the relevant rules. The first rule, obeyed by all three varieties, is that pairs of tubes in that collection must either be nested or disjoint: if they intersect then one must be a subset of the other. Thus the tubes in a tubing (or piping or nesting) are partially ordered by inclusion, and indeed the resulting poset formed by any tubing, nesting, or piping possesses a tree (or forest) as its Hasse diagram. If the elements of a tubing could overlap, that would allow a cycle in the underlying graph of the Hasse diagram.[1]

The fact that the Hasse diagram of a tubing is always treelike allows superstructure to be added: the Hasse tree can be *painted* with colors (usually two main colors). The earliest examples of these superstructures are on the nestings of the linear poset (tubings of the path graph) which naturally label the faces of Stasheff's associahedra [26]. The 2-colored superstructure on these tubings make up the polytopes called multiplihedra [15]. 2-colored structure is generalized to graph tubings in [13], and further to several additional classes of generalized permutohedra in [1], where the results are called lifted generalized permutohedra. Multiplihedra are also seen as shuffles of the generalized permutohedra and generalized to n colors in [11].

The second type of superstructure, which we only briefly mention here, is that the graph of the Hasse diagram of each tubing can be used to define a new building set for an iterated construction of nesting: using pipes (also known as nests), since it is a tree. These 2-fold iterations of the nestings of the path graph make up the cosmohedra, polytopes described in [3] and [2], and generalized to all graphs and posets in [18] and [16].

In this paper we focus on the first type, the colored superstructure, describing a 2-colored version of the poset associahedra of Galashin. The latter were originally defined in [17]. That paper refers to them as P-associahedra, to differentiate them from the poset associahedra defined in [14]. Realizations for Galashin's poset associahedra were found in [25], [20], and [21]. In those sources they are referred to as poset associahedra, but the distinction between the two types of poset associahedra is that the pipes (and pipings) of Galashin's poset associahedra are convex (and *acyclic*), while the original poset associahedra have tubes that are certain *lower sets*, or order ideals, which directly generalize the graph tubings. We'll refer to Galashin's version as *acyclic poset associahedra*, which is also appropriate considering that they are special *acyclonestohedra*. [2] The polytopes we consider in this paper are mapped out in a much broader context in Figure 2.

1.0.1 New polytopes

A colored acyclic tubing has blue, purple and red tubes, and obeys the rule that only blue tubes can be nested inside of blue or purple tubes. These colored tubings form a poset structure. Our main theorem is that for any poset P the colored tubings constitute a polytope: that is, the poset of colored nestings of P is equivalent to a face poset of a polytope, the acyclic multiplihedron. The proof of this theorem will be simplified by the fact that we can rely on earlier results about the graph multiplihedron. Our new acyclic multiplihedra will be cross sections of the graph multiplihedra, and inherit all the nested structure from the tubing structure of the latter.

[1] Allowing overlap of tubes, up to further limitations, moves us into the realm of multitubings and multiassociahedra.

[2] Neither sort of pipes or tubes on posets make a building set on the elements of the poset. In fact they both generalize the building set property in the same way: rather than satisfying the condition that for intersecting tubes their union is found in $\mathcal{B}$, they satisfy the condition that there exists a tube in $\mathcal{B}$ containing that union.

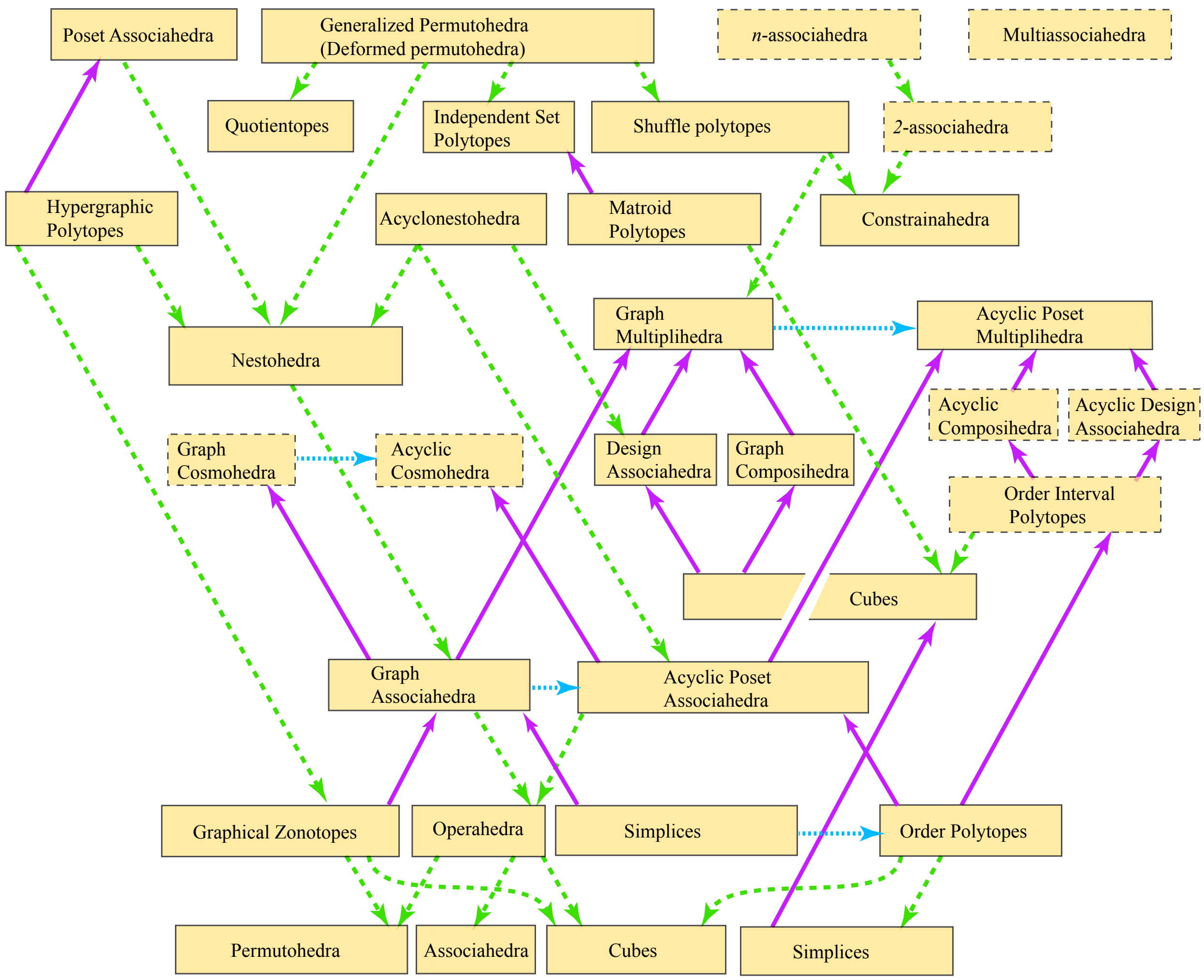

Figure 2: Relationships of families of polytopes: dashed green arrows slope down to indicate subset containment: lower contained in upper. Solid violet arrows point up to indicate lifting: refining the fan, truncation, taking intervals, or extending combinatorial structure. Dashed horizontal arrows show taking a cross section, left to right. Dashed boxes are conjectural polytopes. Many families and relationships were too hard to show here, such as the facts that interval hypergraphic polytopes include the associahedra, and that multiassociahedra include the associahedra, simplices, and certain kinds of amplituhedra.

For details on the relationships shown (and not shown) sources include: for hypergraphic polytopes [6, 7, 5], for poset associahedra [14], for generalized permutohedra and nestohedra [24], for quotientopes [23], for graph multiplihedra and their quotients [13], for generalized multiplihedra, matroid polytopes and independent set polytopes [1], for acyclonestohedra [21], for operahedra [19, 12], for acyclic poset associahedra and order polytopes [17], for 2-associahedra and n-associahedra [8, 4], for shuffle polytopes and constrainahedra [11, 9], for cosmohedra and graph cosmohedra [3, 18, 2], for acyclic cosmohedra [16], and for multiassociahedra [22].

2 Multiplihedra for acyclic poset associahedra.

2.1 Review of graph associahedra and multiplihedra

For a connected graph G a *tube* t is a connected induced subgraph, often given by its set of nodes. Tubes are drawn using closed curves around their nodes when the graph is small enough that the subgraph is easily seen to be thus enclosed. These tubes are uncolored for the graph associahedra, or colored (thick red, thin blue, or dashed purple) for the multiplihedra.

A *tubing* T is a set of tubes of G, each pair nested or disjoint, for which all unions of the tubes in T are induced subgraphs. A *colored tubing* is a tubing of colored tubes, obeying the rule that only blue tubes can be nested inside of blue or purple tubes.

The original motivation for two colors in the combinatorial structures of multiplihedra was to denote domain and range for a function or functor; blue for domain and red for range. We have used actual colors: red, blue, and purple lines—but the red is thick, blue thin, and purple dashed for printing in black and white. The definitions from [13] use the terms thick and thin.

The definitions are subtle, and it can be helpful to note some consequences. For instance the rule that unions must be induced subgraphs means that two tubes in a tubing cannot have tube s contain one node of a graph edge while a disjoint tube t contains the other. The rule that only blue tubes can be nested inside of non-red tubes means that purple tubes never have purple tubes nested inside them.

For a graph G with multiple connected components, we sometimes add that the entire graph G is still considered a tube (despite being disconnected) and thus that the connected components of G cannot all be members of a tubing at once. Alternatively for disconnected graphs we could define the tubings to be any collection of tubings on the connected components; this gives a Cartesian product of tubings on the components. For the rest of this paper we will restrict our attention to the connected graphs, leaving the choice of how to describe disconnected graphs up to practitioner.

The *graph associahedron* $\mathcal{K}(G)$ is defined in [10] as the polytope whose face poset corresponds precisely to the uncolored graph tubings, ordered by reverse inclusion.

The *graph multiplihedron* $\mathcal{J}(G)$ is combinatorially described as the poset of all the colored tubings of a graph. The ordering is given by the following four (covering) relations $U \lessdot V$: tubing U is less than tubing V if:

1. U is achieved by adding a single blue tube to V, which must be added inside another blue or purple tube.

2. U is achieved by adding a single red tube to V, which must be added inside another red tube.

3. U is achieved from V by *resolving* a purple tube of V, by making it blue or red.

4. U is achieved from V by resolving a purple tube of V to red, and simultaneously adding one or more purple tubes just inside of that new red tube (and not inside any other tube).

Relations in the poset of colored tubings thus generated can be difficult to determine. Simply being subsets of the tubes (of each color) does not make one colored tubing comparable to another. For instance,

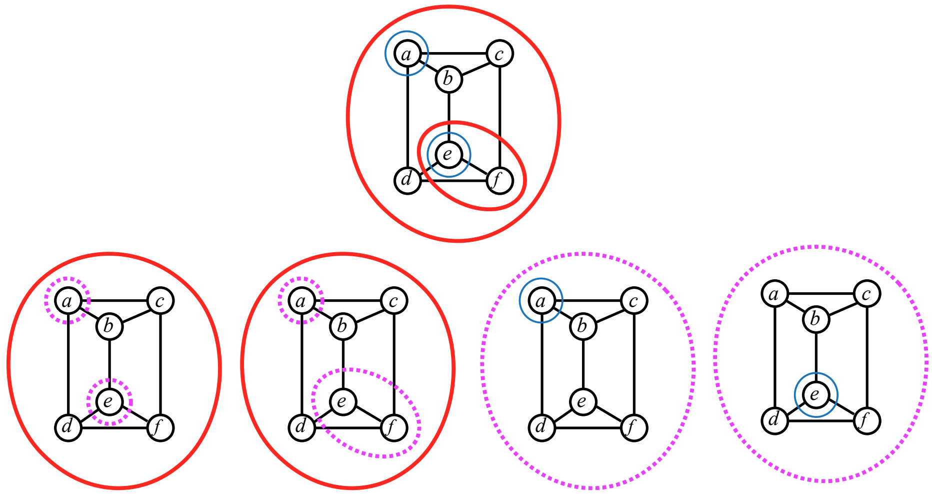

Figure 3: A colored tubing and some of the facets that contain it. All four of these facet tubings are induced by acyclic pipings of the double-claw poset in Figure 6.

starting with a single universal red tube, the only tubings less than that one must have all red tubes, since there is no way to legally add blue or purple tubes. The same is true for the single universal blue tube: and these two examples are facets of the resulting polytope that are in fact equivalent to the graph associahedron for the same graph.

The minimal elements are those tubings with a maximal number of tubes, some red and some blue tubes, no purple. The maximal number of tubes is always n, the number of nodes. Thus we can associate an element of the poset with the maximal nestings that it can be extended to become, so that we have $U \prec V$ when the n-tube tubings that U can become is a subset of those that V can become. The maximal element of the entire poset is the tubing with one universal purple nest. Then by adding a single blue tube inside it, or resolving it to blue, or by resolving it to red, and perhaps adding any allowable purple tubes inside it, we see the penultimate elements of the poset which correspond to facets of our face poset.

A unifying principle behind the relations we have listed is that they describe the resolution of a colored tree into a binary tree, with simplest coloring. Ardila and Doker point out in [1] that the Hasse diagram of a tubing, a tree, can have its edges painted with two colors. Red at the root, and blue at the leaves, the rule for painting is that blue must be above red: purple tubes correspond to nodes where red and blue meet at a branch point of the tree. Then the covering relations can be expressed as resolving the tree until it is binary with no bi-colored branch points.

2.1.1 Multiplihedron facet realization

Let G be a connected graph with vertices $v_1, \ldots, v_n$. It is shown in [13] that $\mathcal{J}(G)$ is the poset of faces of an n-dimensional convex polytope with vertices corresponding to the colored tubings of n tubes, where n is the number of nodes of G. In [13] is given a geometric realization of the graph multiplihedron for any graph G with n nodes. The polytope is full dimensional, in $\mathbb{R}^n$ where coordinate x_i corresponds to node v_i of G. The facet inequalities for the polytope come in two flavors:

1. For each colored tubing of G with only one blue tube t, a lower facet given by

$$\sum_{v_i \in t} x_i \geq 3^{|t|-1}.$$

2. For each colored tubing of G with only one red tube G itself, and (possibly) k purple tubes $t_1 \dots t_k$, an upper facet given by:

$$\sum_{v_i \notin t} x_i \leq 3^n - \sum_{j=1}^{k} 3^{|t_j|}.$$

2.1.2 Multiplihedron vertices

In [13] it is shown that the vertices of this polytope are given by the following assignment of values to the coordinates x_i for an n-tube tubing T with all red and blue tubes (thus maximal as a tubing, so minimal in the poset of tubings). For a node v_i of G there will be a tube $\epsilon(v_i)$ that is the smallest containing v_i. For any tube t there may be some tubes s that are nested inside t and inside no other tube: we say $s \prec t$ in the containment order.

1. For $\epsilon(v_i)$ a blue tube we have:

$$x_i = 3^{|\epsilon(v_i)-1|} - \sum_{s \prec \epsilon(v_i)} 3^{|s|-1}.$$

2. For $\epsilon(v_i)$ a red tube we have an extra factor of 3:

$$x_i = 3^{|\epsilon(v_i)|} - \sum_{s \prec \epsilon(v_i)} 3^{|s|}.$$

Example calculations of some coordinates associated to nodes of a graph with a maximal colored tubing are shown in Figure 13.

2.2 Review of acyclic poset associahedra

We will work with connected posets P, which means that the Hasse diagram of P is a connected graph. A convex subposet is a subposet C such that if $a \in C$ and $b \in C$, with $a \leq x \leq b$, then $x \in C$. We often call a convex subposet *acyclic*, since a non-convex subposet has the property that collapsing it to a single element in the Hasse diagram results in the remaining directed edges of the Hasse diagram forming a directed cycle, after the collapse. Similarly, we say a collection of subposets is acyclic if collapsing all subposets in the collection simultaneously results in no directed cycles.

Partitions of the elements of the poset into connected parts, which are acyclic (and thus must have acyclic parts) label the faces of a polytope called the *order polytope* $\mathcal{O}(P)$. This polytope first defined by Stanley for posets with unique maximum and minimum elements, and more generally for all posets by Galashin in [17]. Galashin's order polytopes are found combinatorially as faces of Stanley's, via adjoining a max and min if needed. The acyclic partitions are ordered by reverse refinement, with the partition into all singletons as the interior of the polytope and the trivial partition not included as a face: it can be considered the minimal element in the face lattice.

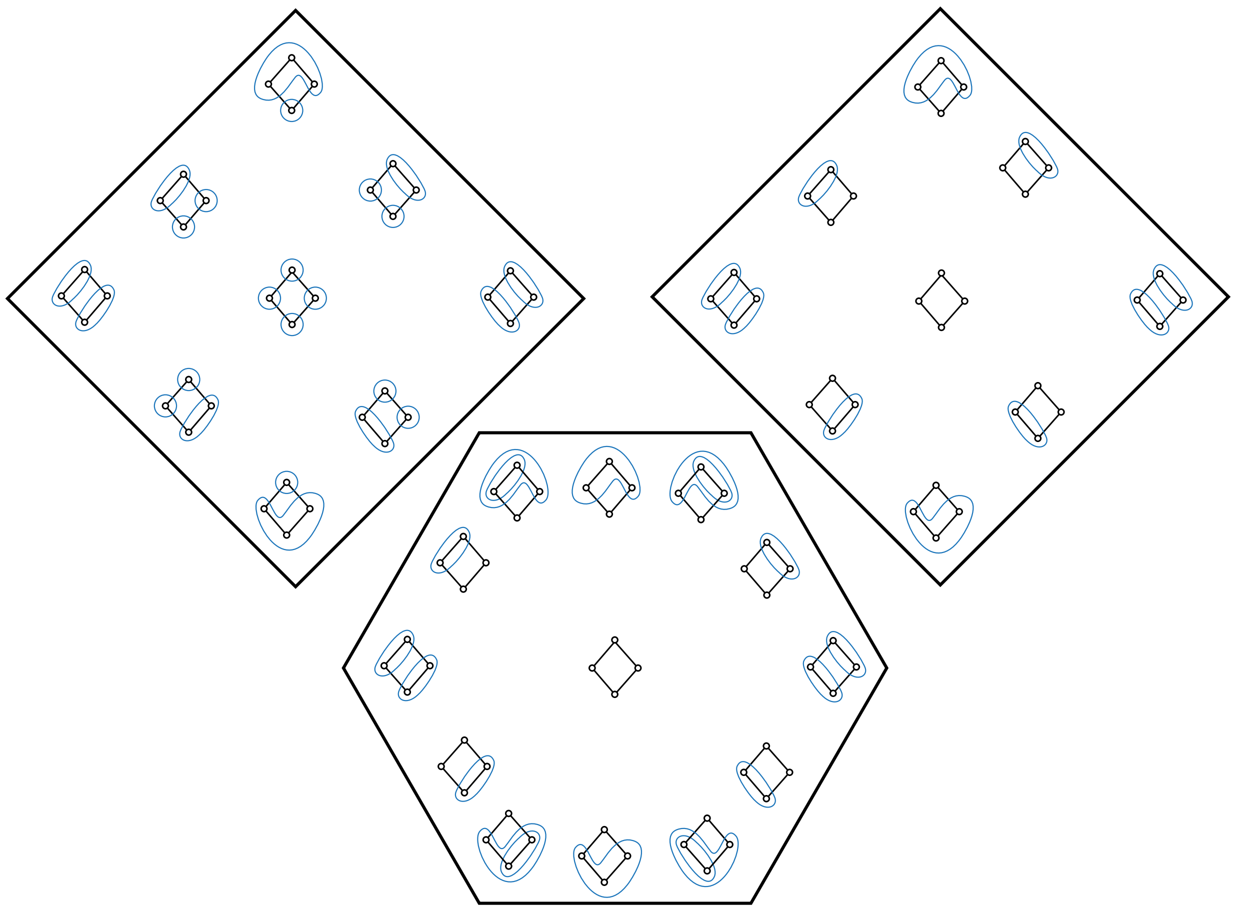

Figure 4: On the left is the order polytope $\mathcal{O}(P)$ for the diamond poset. On the right is the same order polytope, showing only subposets of size greater than one. Two of the vertices are truncated, thus promoted to new facets of the acyclic poset associahedron in the center.

For a connected poset P we consider *pipings* as described in [17]. A pipe N of P is a connected convex subposet of P with at least two nodes. That is the same as a connected induced acyclic subgraph of the Hasse diagram of P with at least one edge. A piping $\mathcal{N}$ is a set of pipes such that each pair is nested or disjoint, and such that the collection of those pipes is also acyclic.

The acyclonestohedron of the poset $\mathcal{A}(P)$ is a polytope whose face poset is the same as the collection of pipings, ordered by reverse inclusion. See Figure 4 for the full poset of pipings on a diamond poset, and Figure 5 for the facet pipes on a post with five elements. The lower dimensional faces are then labeled by the piping that is found by collecting the pipes for the facets containing that lower dimensional face.

The acyclonestohedron for a poset is the (acyclic) poset associahedron. It is shown in [17] that this polytope exists as a truncation of the order polytope $\mathcal{O}(P)$. Truncating a face promotes it to a new facet. The full iterative procedure is described in [17]in terms of stellations of the polar dual polytope. The stellations, or dually the truncations, must proceed in order of dimension of the face to be steallated or truncated. The promoted faces are those for which the adjacent facets of $\mathcal{O}(P)$ are labeled by edges of the Hasse diagram which can together constitute a single pipe. See Figure 4 for the process on a polygon, and Figure 15 for the order polytope and the realization (via facet inequalities given in the next section) that exhibit the truncations on the order polytope which result in the example shown in Figure 5.

Notice that a piping does not have to obey the requirement that the union of its pipes is an induced graph, in fact the edges of the derived graph achieved by collapsing the piping are often formed when there is an edge (a covering relation of P) between two nests of the nesting. However, when we take the line graph L of the Hasse diagram, each pipe of P corresponds to an *induced* tube of L: the edges of the pipe are the nodes in that tube. Moreover, a piping of the poset becomes a tubing of the line graph, via the direct translation: if an edge of the Hasse diagram is in a pipe of the piping, then the corresponding node of the line graph is in the corresponding tube of the induced tubing. The tubes will be compatible, either nested or non-adjacent due to the line graph construction. Of course since only acyclic collections of pipes are allowed, not all tubings of the line graph are recovered in this way from pipings of the Hasse diagram. In fact, in [20] the authors discovered that the acyclonestohedron for P is realized as a cross section of the graph associahedron for the line graph of the Hasse diagram.

2.3 Acyclic Multiplihedra

Using the correspondence between pipings and induced acyclic tubings, it is straightforward to define the 2-colored version of the acyclonestohedra: the acyclic multiplihedra.

Definition 1. For a poset P we define the colored pipings on P as pipings with blue, red, and purple pipes, such that the induced colored tubing on the line graph of the Hasse diagram is a colored tubing of that line graph. Thus all the same requirements hold: a colored piping is just a special colored tubing, and the colored pipings are ordered via the same relations of adding or resolving colored tubes.

For example, we show a colored piping and its induced colored tubing on the line graph, in Figure 6. The poset of colored pipings for a poset P is called the acyclic multiplihedron $\mathcal{J}(P)$.

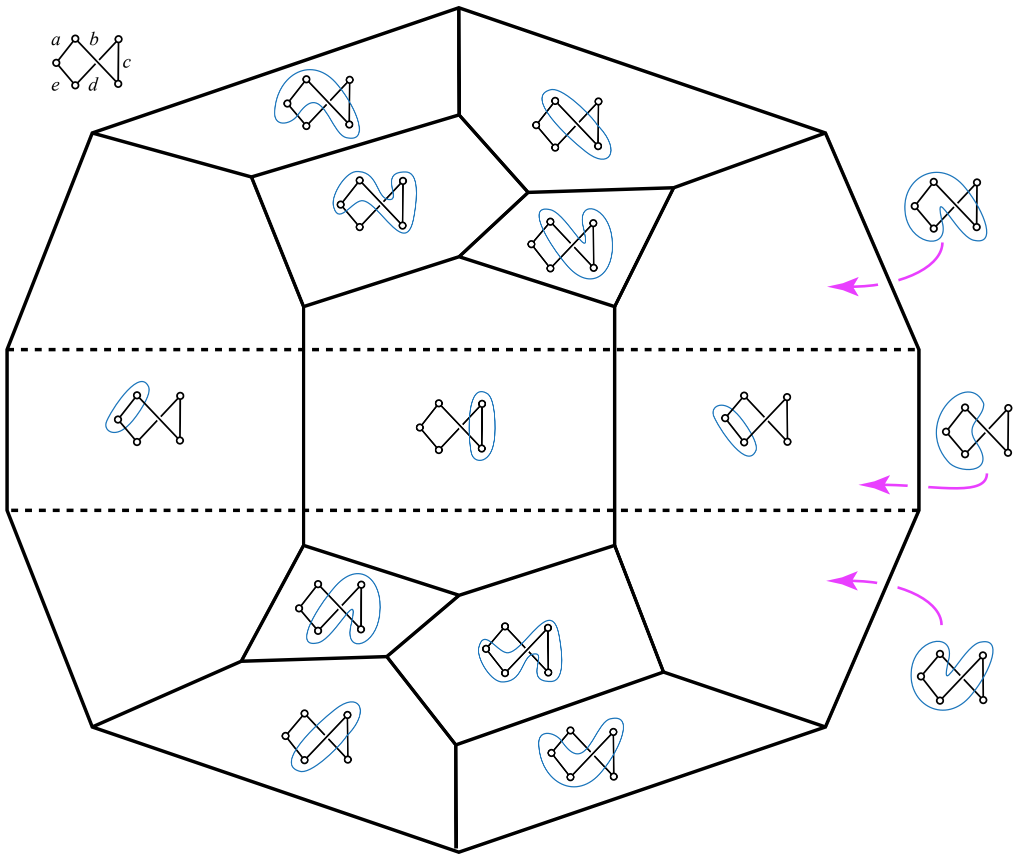

Figure 5: Acyclonestohedron. Specifically, the acyclic poset associahedron for the poset with Hasse diagram shown. Facets are labeled by pipes: tubes that are connected convex subposets. Figure 15 shows the order polytope for this poset, and the geometric realization of this acyclic poset associahedron.

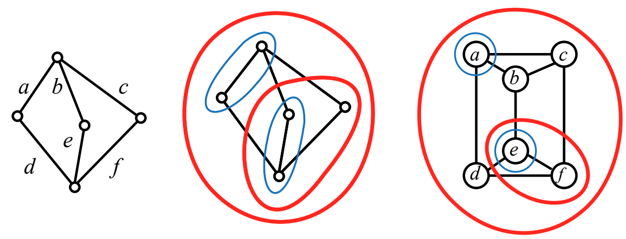

Figure 6: A colored piping on the poset with Hasse diagram at left, and its induced colored tubing on the line graph of that Hasse diagram, on the right. Some facet tubings induced by pipings that contain this piping are shown in Figure 3, and several maximal tubings with coordinates calculated are shown in Figure 13.

Theorem 1. *The colored pipings of a poset P with n nodes correspond to the face poset of a convex polytope $\mathcal{J}(P)$ of dimension $n-1$.*

Proof. The proof is via an explicit geometric realization, which we will describe and prove in the next section. The summary is that the acyclic poset multiplihedron is a geometric cross section of the graph multiplihedron of the line graph of the Hasse diagram. □

For examples: the vertices and some faces of the acyclic multiplihedron polytope for the bowtie poset are shown in Figure 7, also pictured in Figure 1. The acyclic multiplihedron for the diamond poset with labels is shown in Figure 8.

Recall that for a Hasse diagram that is a tree, with no cycles, the acyclic poset associahedron is called the operahedron [19]. It is the graph associahedron of the line graph of the Hasse diagram. Similarly we have the following:

Corollary 1. *A poset P whose Hasse diagram has no cycle (every edge is a bridge) has acyclic multiplihedron which is the graph multiplihedron of the line graph of the Hasse diagram of P.*

The acyclic multiplihedron for the three-edge claw poset with labels is shown in Figure 10. It is an operahedron, specifically the permutohedron.

2.4 Realization

To realize the acyclic multiplihedron as a convex hull we will start with the same set of facet inequalities as for the graph multiplihedron of the line graph of the Hasse diagram. To those we add an equality for each cycle in the Hasse diagram: choosing a direction to follow that cycle we add the coordinates whose covering relation agrees with that direction and subtract the ones which do not, setting the total equal to zero.

Looking ahead, the proof that these inequalities and equalities together give a realization of the acyclic multiplihedron will rely on the fact that only acyclic facet tubings will intersect with the hyperplane defined by the cycle equalities. Therefore we note that there is a practical choice between efficiency in constructing the realizations for posets. One can either include an inequality for every upper and lower tubing of the line graph, or just for those tubings which use only tubes that are convex in terms of the poset. The latter is faster for constructing a single example, but if you have several posets with the same underlying line graph of all

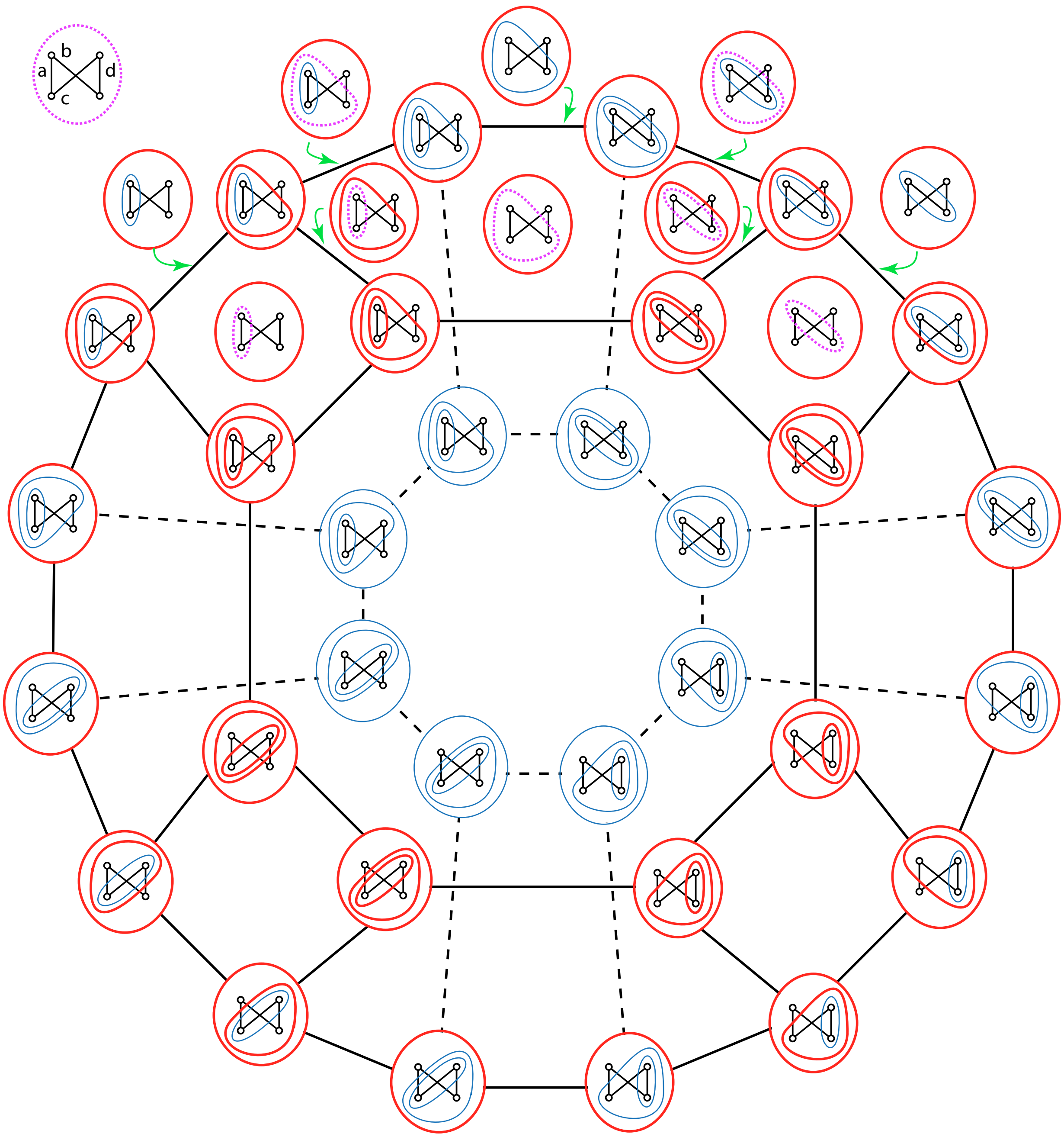

Figure 7: Multiplihedron for bowtie poset, showing all the vertices and some additional face labels. The f-vector is $(32, 48, 18)$.

their Hasse diagrams, you can keep all the same inequalities and change only the cycle equalities to quickly realize them all.

1. For each colored piping of P with only one blue nest t, a lower facet given by

$$\sum_{v_i \in t} x_i \geq 3^{|t|-1}.$$

2. For each colored piping of P with only one red nest P itself, and (possibly) k purple nests $t_1 \ldots t_k$, an upper facet given by:

$$\sum_{v_i \notin t} x_i \leq 3^n - \sum_{j=1}^{k} 3^{|t_j|}.$$

3. For each cycle c in the Hasse diagram, an equality. Choosing an arbitrary direction to traverse the cycle, the orientation (covering relation) of the edge v_i in c will either agree with or be against the direction of traversal of c.

$$\sum_{v_i \text{ with } c} x_i - \sum_{v_i \text{ against } c} x_i = 0$$

   Following [20] we will refer to the intersection of all the cycle equalities as the *evaluation space* for the poset.

Examples: Table 1 shows the realization for the diamond poset, using variables (x_a, x_b, x_c, x_d) with subscripts from the edges of the diagram in Figures 8 and 9. The upper facets are in the foreground of those figures, and the lower facets in the background. We list the unused facets of the full 4D cycle-graph multiplihedron for comparison. The choice of positive and negative for the coefficients is $x_a - x_b + x_c - x_d = 0$ so of course the single cycle equality can be multiplied by -1.

lower facets	upper facets	unused facets
$x_a \geq 1$	$x_a + x_b \leq 72$	$x_a \leq 54$
$x_b \geq 1$	$x_c + x_d \leq 72$	$x_b \leq 54$
$x_c \geq 1$	$x_a + x_d \leq 75$	$x_c \leq 54$
$x_d \geq 1$	$x_b + x_c \leq 75$	$x_d \leq 54$
$x_a + x_b \geq 3$	$x_a + x_b + x_c \leq 78$	$x_a + x_c \leq 72$
$x_c + x_d \geq 3$	$x_b + x_c + x_d \leq 78$	$x_b + x_d \leq 72$
$x_a + x_b + x_c + x_d \geq 27$	$x_a + x_b + x_d \leq 78$	$x_a + x_b + x_c \geq 9$
	$x_a + x_c + x_d \leq 78$	$x_a + x_b + x_d \geq 9$
	$x_a + x_b + x_c + x_d \leq 81$	$x_a + x_c + x_d \geq 9$
cycle equality		$x_b + x_c + x_d \geq 9$
$x_a - x_b + x_c - x_d = 0$		$x_a + x_c \geq 3$
		$x_b + x_d \geq 3$

Table 1: The realization for the diamond poset acyclic multiplihedron, using variables (x_a, x_b, x_c, x_d) with subscripts from the edges of the diagram in Figure 8. Facet labels are shown in Figure 9. An image of the realization is in Figure 11.

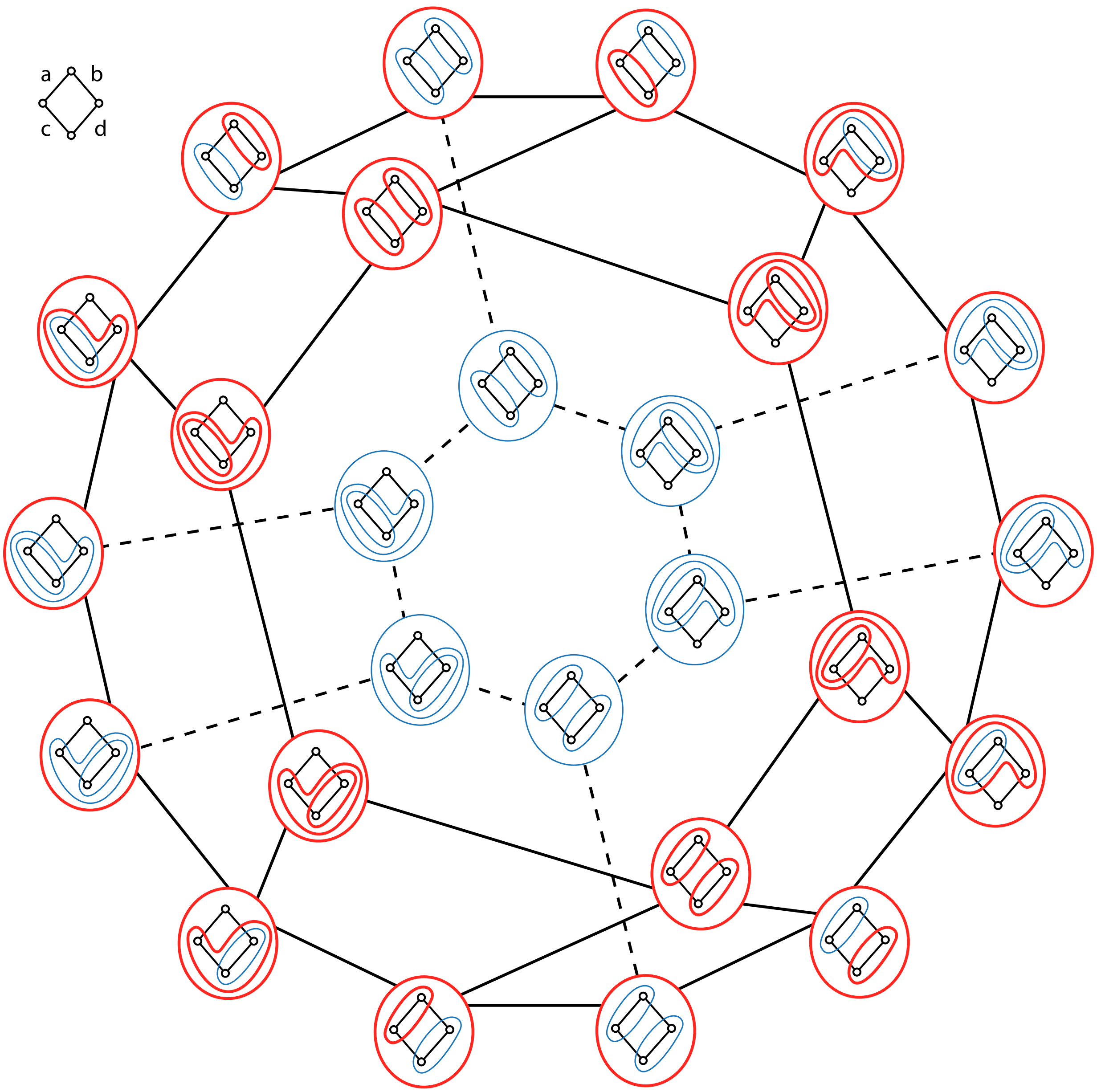

Figure 8: Multiplihedron for diamond poset. The f-vector is $(26, 40, 16)$.

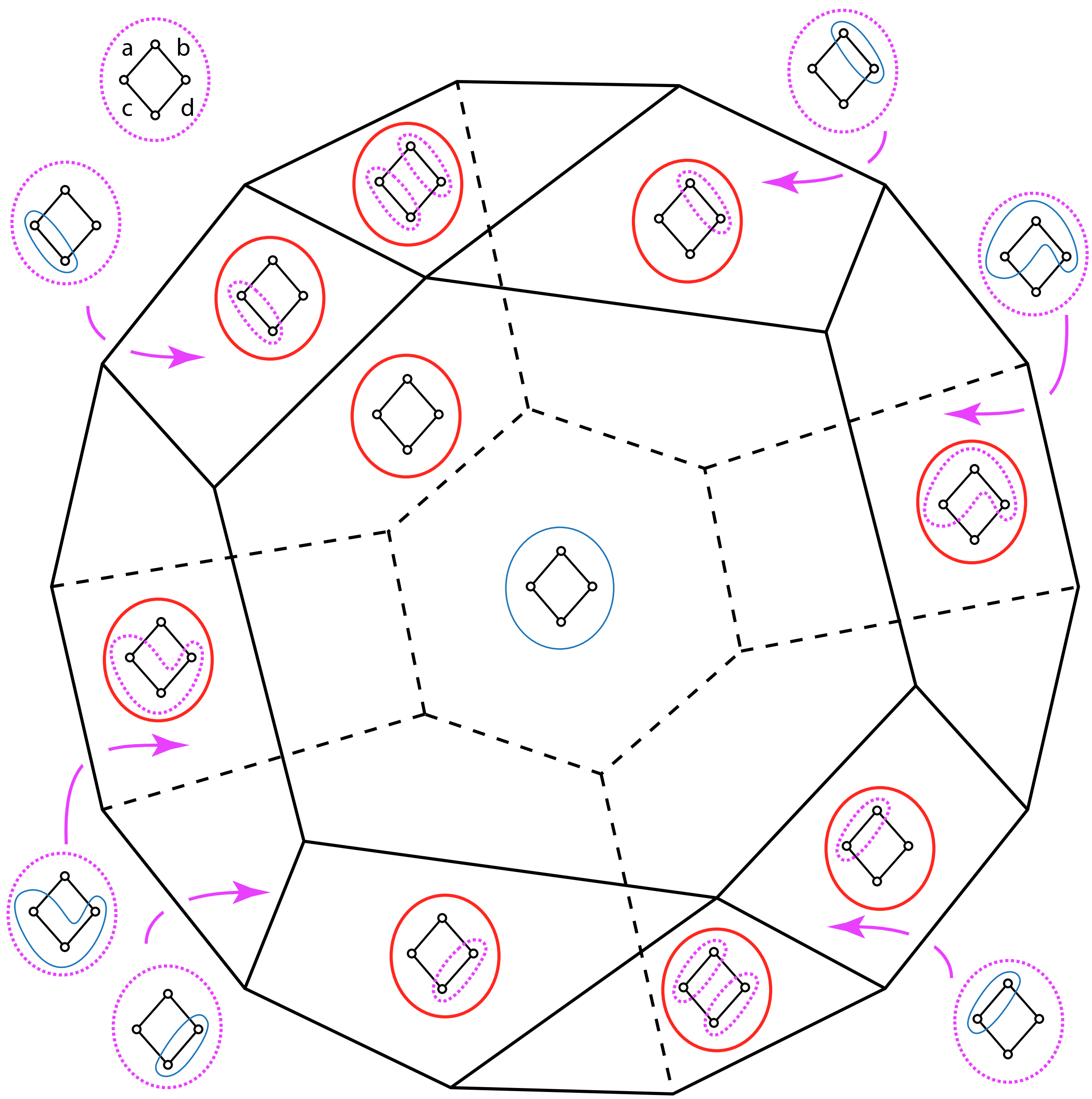

Figure 9: Multiplihedron for diamond poset, showing facet labels for the calculations in Table 1.

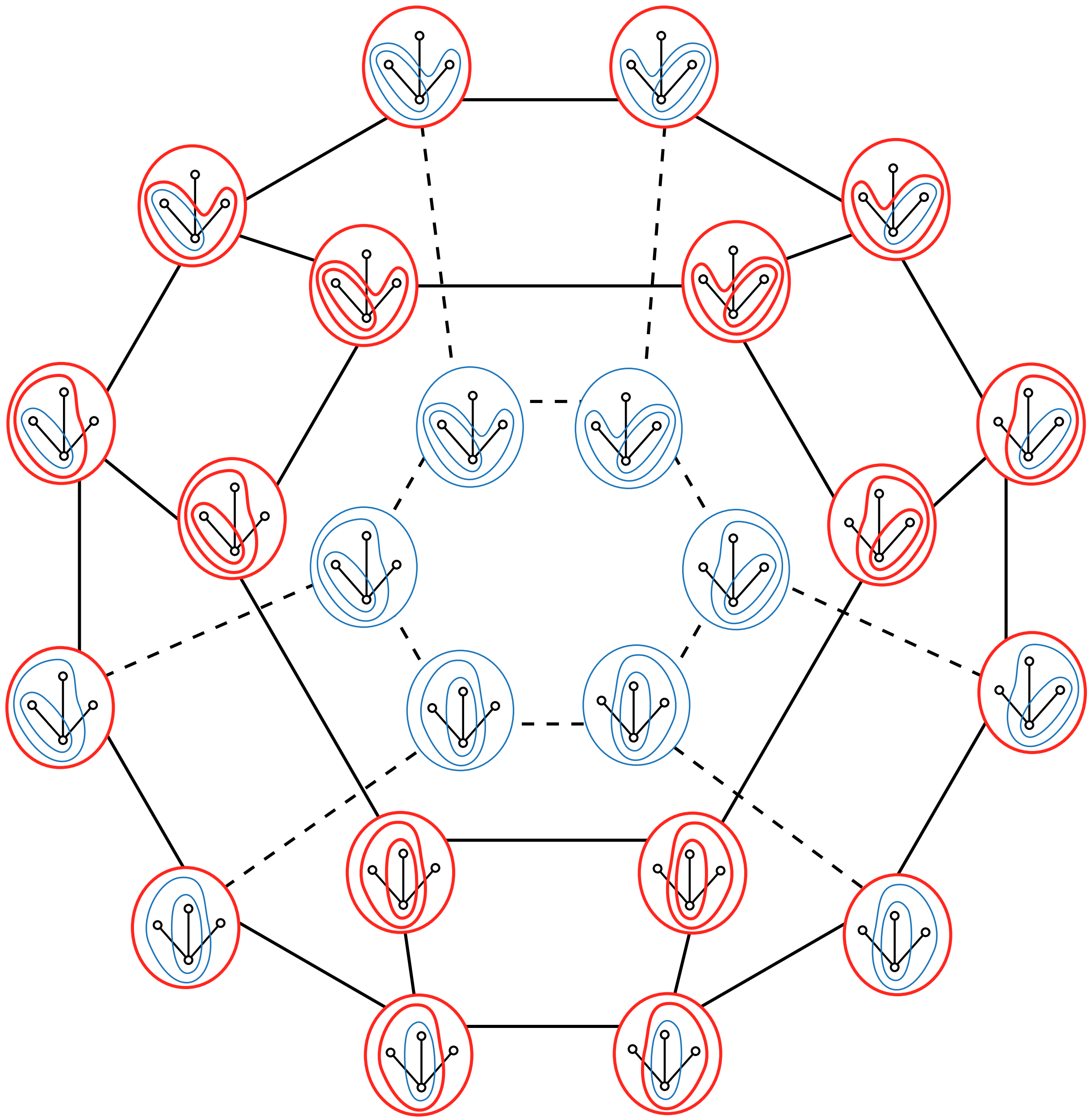

Figure 10: Multiplihedron for claw poset. The f-vector is $(24, 36, 14)$. Since the Hasse diagram is a tree, this is precisely the multiplihedron for its line graph, the complete graph on three vertices. Thus it is a 3D permutohedron, as shown in [13].

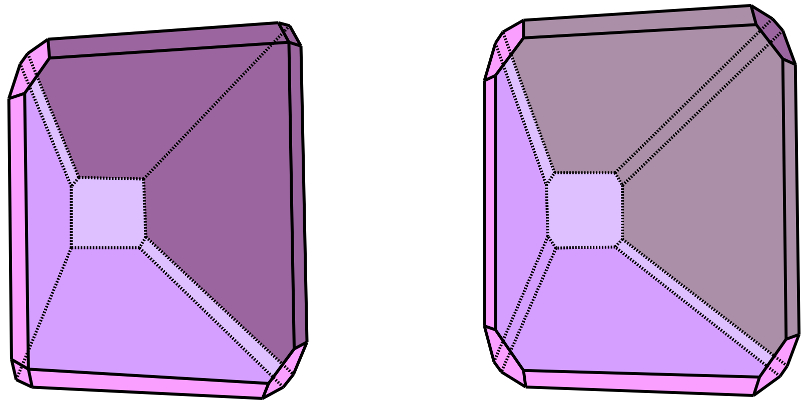

Figure 11: On the left: acyclic multiplihedron realization for the diamond poset, as seen in Figure 8. On the right: acyclic multiplihedron realization for the bowtie poset, as seen in Figure 7.

Table 2 shows the realization for the bowtie poset, using variables (x_a, x_b, x_c, x_d) with subscripts from the edges of the diagram in Figure 7. The upper facets are in the foreground, and the lower facets in the background. We list the unused facets of the full 4D cycle-graph multiplihedron for comparison.

lower facets	upper facets	unused facets
$x_a \geq 1$	$x_a + x_b \leq 72$	$x_a \leq 54$
$x_b \geq 1$	$x_c + x_d \leq 72$	$x_b \leq 54$
$x_c \geq 1$	$x_a + x_c \leq 72$	$x_c \leq 54$
$x_d \geq 1$	$x_b + x_d \leq 72$	$x_d \leq 54$
$x_a + x_b \geq 3$	$x_a + x_b + x_c \leq 78$	$x_a + x_d \leq 75$
$x_c + x_d \geq 3$	$x_b + x_c + x_d \leq 78$	$x_b + x_c \leq 75$
$x_a + x_c \geq 3$	$x_a + x_b + x_d \leq 78$	$x_a + x_b + x_c \geq 9$
$x_b + x_d \geq 3$	$x_a + x_c + x_d \leq 78$	$x_a + x_b + x_d \geq 9$
$x_a + x_b + x_c + x_d \geq 27$	$x_a + x_b + x_c + x_d \leq 81$	$x_a + x_c + x_d \geq 9$
		$x_b + x_c + x_d \geq 9$
cycle equality		
$x_a - x_b - x_c + x_d = 0$		

Table 2: The realization for the bowtie poset acyclic multiplihedron, using variables (x_a, x_b, x_c, x_d) with subscripts from the edges of the diagram in Figure 7. An image of the realization is in Figure 11.

2.5 Proof of the realization

We will show that the combinatorial description of the acyclic poset multiplihedra is realized by the geometric realization we give above.

The proof follows the same logic as in [20], in which the authors show that the acyclonestohedra themselves are found as cross sections of a geometric realization of certain graph associahedra. Given a poset with its Hasse diagram, they take the line graph of that Hasse diagram and a realization of the associahedron of that line graph. Then they add equalities for each cycle in the original Hasse diagram; together the intersection of these equalities defines what they call the evaluation (sub)space. The intersection of this evaluation space with the graph associahedron is shown to be the acyclonestohedron. The proof proceeds by showing that a face of the graph associahedron intersects all the hyperplanes in the evaluation space if and only if that face corresponds to a tubing which arises from an acyclic tubing (piping) of the Hasse diagram. This demonstrates the desired geometric realization simply because the structure of the acyclonestohedron is precisely the structure of the graph associahedron (of the line graph of the Hasse diagram), restricted entirely to the acyclic faces.

Our proof will follow that logic exactly: starting with a realization of the graph multiplihedra. Thus the proof requires two lemmas: first that any face which corresponds to a not-acyclic tubing (so cyclic!) has its vertices all on one side of the evaluation space, so that the face itself does not intersect the evaluation space at all. The proof of this lemma will be checking that our vertex coordinates obey the correct inequalities: if not acyclic then all associated vertex evaluations will be all greater than (or all less than) at least one of the cycle equalities.

The second lemma is that any face which corresponds to an acyclic tubing does in fact intersect the evaluation subspace. For that to be true, we need such a face to have its set of vertices distributed around the evaluation space, to ensure that the face is cut by that space. Specifically, the set of vertices must include points that reside in each chamber of the central hyperplane arrangement whose common intersection is the evaluation space. In terms of the oriented matroid, the chambers are represented by sign vectors using the symbols $\{+, -\}$ to refer to the position relative to each of r oriented hyperplanes.

This we will demonstrate just by considering an acyclic face, and showing how to construct its vertices that lie in each chamber. The same basic fact supports both our lemmas: if a tubing of the line graph is acyclic, it must be relatively small, with several different (usually cyclic) ways to extend it to a maximal (vertex) tubing of the multiplihedron. Conversely, if the tubing is already cyclic, it is large enough that the extensions are all similar, in fact all on one side of a hyperplane.

Lemma 1. *Let F_T be a face of the graph multiplihedron associated to a non-acyclic tubing T of the line graph of the Hasse diagram of a poset P. Then for some cycle c of the Hasse diagram of P all the vertices in F_T lie on one side, in the same halfspace, of the hyperplane associated to that cycle.*

Proof. All the vertices of F_T will be extensions of T via adding red or blue tubes and resolving any purple tubes. Let c be a cycle of the Hasse diagram on which T exhibits its non-acyclic character. Then the non-acyclic tubing T must have either a tube t which is not convex (involving c, so containing part of c but failing convexity via c):, or a set of non-nested tubes which is not acyclic, again involving c. In the first case, t is a single pipe which contains all the edges of one orientation of c (up or down in the Hasse diagram) but not all the edges of c of the other orientation. Recalling that edges are nodes of the line graph, that means there are some nodes outside of t but part of c.

The cycle equality for c can be rearranged: $\sum_{v_i \text{ with } c} x_i = \sum_{v_i \text{ against } c} x_i$ Now we consider evaluating the left hand side of that cycle equality for c. Choosing the traversal of c to be in the direction of the edges contained in t we see the inequalities:

$$\sum_{v_i \text{ with } c} x_i \leq \sum_{v_i \in t} x_i < \sum_{v_i \in (c-t)} x_i \leq \sum_{v_i \text{ against } c} x_i.$$

The second inequality above is due to the formulas, from Section 2.1.2, for x_i in a vertex (maximal) tubing. Since the values assigned to the nodes (edges of the Hasse diagram) grow as powers of base 3 with their proximity to the exterior universal tube, then the value of any x_i outside a tube is larger than the sum of the values inside it. That follows from the basic inequality: $3^k + 3^m < 3^{k+m+1}$, for $k, m \geq 0$. (Note, that doesn't work for base 2, since $2^0 + 2^0 = 2^1$.)

For a node v_i of G there will be a tube $\epsilon(v_i)$ that is the smallest containing v, and just as for any tube there may be some tubes that are nested inside it and inside no other tube: $t \lessdot \epsilon(v_i)$ in the containment order. Thus the cycle equality fails, strictly, so that any vertex of the face of the tubing T must lie on the same side of the cycle hyperplane, so that F_T does not intersect the evaluation space.

The inequalities are similar for the case in which T has a set of non-nested tubes $t_1, \ldots, t_k$ whose union is non-acylic with respect to c. Here the set of non-nested tubes contains all the edges of one sign given an orientation of c but not all the edges of the other sign. Recalling that edges are nodes of the line graph, that means there are some nodes outside of the union but part of c. Choosing the traversal of c to be in the direction of the edges contained in the union we see the inequalities:

$$\sum_{v_i \text{ with } c} x_i \leq \sum_{j=1}^{k} \sum_{v_i \in t_j} x_i < \sum_{v_i \in (c - \bigcup t_j)} x_i \leq \sum_{v_i \text{ against } c} x_i.$$

Notice that the colors of the tubes involved do not change either inequality, since red tubes (which contribute an extra factor of 3) can only be inside red tubes.

Example: Figure 12 shows a pair of pipings that demonstrates the inequalities for Lemma 1. Next to each non-acyclic piping T is a maximal tubing that corresponds to a graph multiplihedron vertex in the facet F_T. On the top row the inequality is

$$x_1 + x_3 + x_7 + x_8 \leq x_1 + x_2 + x_3 + x_7 + x_8 < x_4 + x_5 + x_6 \leq x_2 + x_4 + x_5 + x_6.$$

On the bottom row the inequality is

$$x_1 + x_3 + x_7 + x_8 \leq x_1 + x_3 + x_7 + x_8 < x_2 + x_4 + x_5 + x_6 \leq x_2 + x_4 + x_5 + x_6.$$

□

Lemma 2. *Let F_T be a face of the multiplihedron associated to an acyclic tubing T of the line graph of the Hasse diagram of P. Then F_T intersects the evaluation space, which is the intersection of all the cycle hyperplanes.*

Proof. Let F_T be a face of the multiplihedron associated to an acyclic tubing T of the line graph of $H(P)$. The face F_T is given by the intersection of the facet hyperplanes of the multiplihedron which contain that face, one for each tube of T.

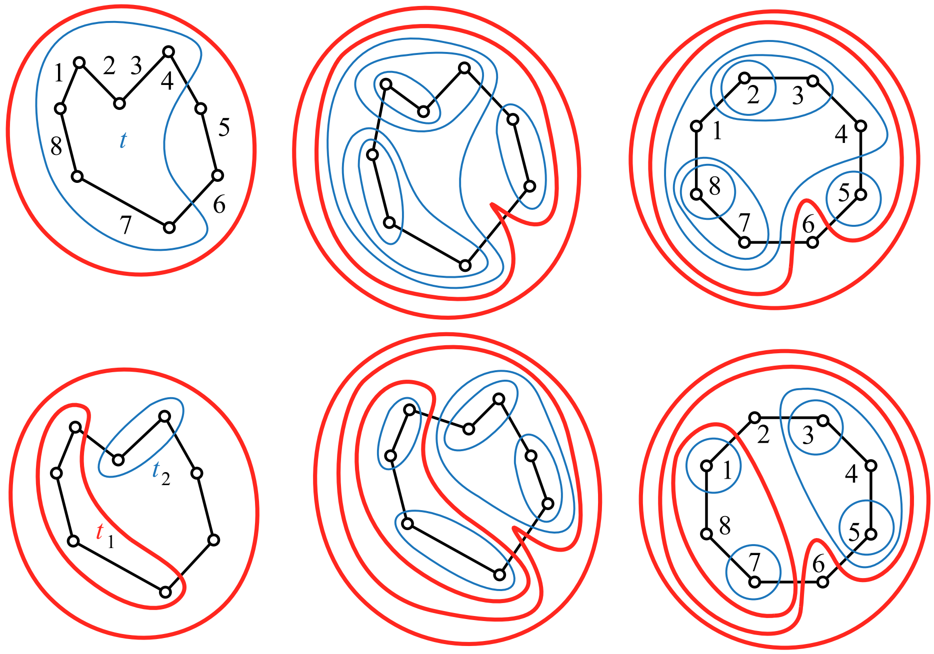

Figure 12: Pipings to demonstrate a non-convex pipe t (top row) and a non-acyclic piping with t_1, t_2 (bottom row). The tubings (in the middle and right) are vertex tubings of the graph multiplihedron, first drawn as pipings of the edges of the poset, then as tubings of the line graph.

The number of cycle hyperplanes is the same as the number of independent cycles in the Hasse diagram, the cycle rank: $r = |E| - n + 1$ for a connected diagram of n nodes. (Kirchoff's cyclomatic number.) Notice that combining the equations of cycles gives a new cycle equation. We choose independent cycles by selecting a minimum set of edges that need to be removed to make the graph a tree, and then pick one cycle for each of those edges. The number of tubes in T is at most $n - 1$ red and blue, including the universal tube, since we are considering an acyclic tubing of an n-node poset. Each face of the graph multiplihedron is determined by one equation for each tube. (There may be many more facets which contain that face, but one for each tube is sufficient to determine that face.) Thus the total number of equations in the realization of a face is at most $|E|$, the number of edges of the Hasse diagram.

Note: the equations themselves are of course not unique, they can be replaced by combinations of themselves with others, that is, row operations. We often add together independent cycles or subtract tube equations. Via the latter, we can get a set of equations for tubes where each variable has a non-zero coefficient only once, as in Definition 18 of [13].

The cycle equalities thus chosen are linearly independent and there are fewer of them than the dimension we are working in, which is $|E|$, the number of edges in the Hasse diagram. Thus the number of chambers is exactly 2^r, where $r = |E| - n + 1$. These chambers have all possible sign vectors of r components from $\{+, -\}$. To find any vertex of our face F_T combinatorially we have to add tubes to T until we get the max number of red and blue tubes, which is $|E|$. So in the case where we have a maximal acyclic poset tubing T, we need exactly r more red and blue tubes to get $|E|$ of them.

So we need to add tubes so that each choice of tube determines a +, or − , that is, the point obeys an inequality > or < for each of the cycle hyperplanes. We claim that the final calculation of the coordinates from the maximal tubings will achieve all the combinations of > and < for the cycle equalities. In the case where we have fewer than $n-1$ tubes in T, we start by arbitrarily adding more (and resolve some purple tubes) to get a maximal acyclic tubing.

Given the maximal acyclic tubing T, for each cycle c of the Hasse diagram there will be a pair of edges of the Hasse diagram neither of which are the only edge of a single tube, but are either both in or both out of every tube in T. Furthermore, in each pair, given a traversal of the cycle, one edge will be oriented with the direction of the traversal, and the other against. These pairs might overlap, sharing an edge between several pairs, specifically when cycles overlap. Choosing exactly one edge from each pair and deleting it produces a spanning tree; and this choice determines a cycle basis for the evaluation space. Taking that collection of cycles and considering its hyperplanes, we claim there is a vertex of F_T from the graph multiplihedron in each chamber of the central arrangement. The claim follows since the collection of edges in the pairs mentioned are nodes in the line graph that can be completely ordered in nested depth via the additional tubes (in groupings of these nodes that correspond to cycles sharing an edge.) Furthermore, for each pair of edges we can choose the tubes to make either edge in the pair at a greater nested depth, and that is a decision independent of the options chosen for the other pairs. Then for any hyperplane of the chosen cycle basis, we can (independently of the other hyperplanes) force the vertex to lie on either side of it, due to the exponential growth of the coordinate values as nested depth decreases. Examples follow; note that the color of the added tubes again preserves the inequalities needed since the blue tubes cannot be outside of red, and the red tubes confer an extra factor of 3. □

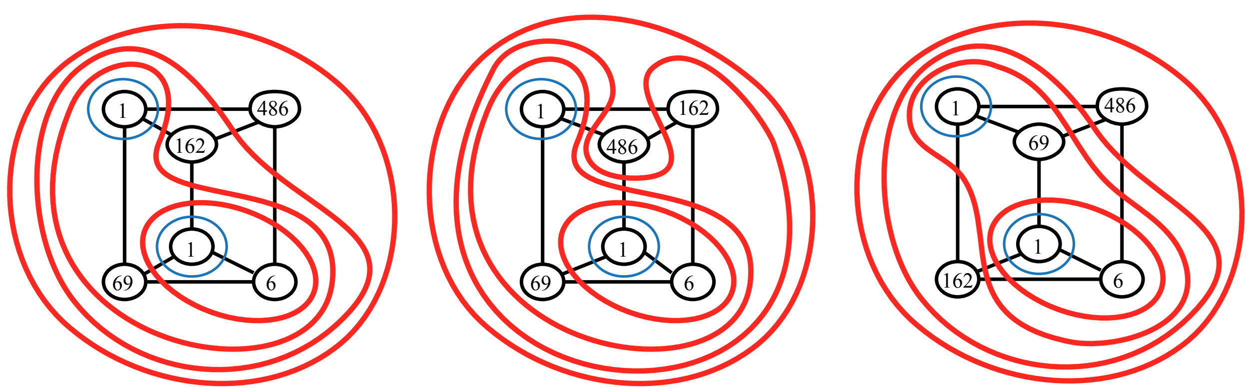

Figure 13: Examples of values assigned to the variables associated to each node in some maximal colored tubings, in the realization of the graph multiplihedron for the graph shown. These are specifically three ways to add tubes to the maximal acyclic poset tubing in Figure 6 to get a maximal graph tubing.

Examples: Figure 6 shows a maximal acyclic piping on P the double claw poset with six covering relations shown. The same piping is shown as a tubing of the line graph of the Hasse diagram, and in Figure 13 are shown three of six vertex tubings of the graph multiplihedron found by adding tubes to that tubing. The leftmost can be checked to obey the inequalities: $x_a + x_d < x_b + x_e < x_c + x_f$ which lies in the chamber designated $< -, - >$, using the two hyperplanes $x_a + x_d = x_b + x_e$ and $x_b + x_e = x_c + x_f$. The center obeys $x_a + x_d < x_b + x_e > x_c + x_f$ which lies in the chamber designated $< -, + >$. The right obeys $x_a + x_d > x_b + x_e < x_c + x_f$ which lies in the chamber designated $< +, - >$. The fourth maximal tubing needed to lie in the chamber $< +, + >$ is left to the reader. A larger example is shown in Figure 14, to see the pairs of edges that can occur in a maximal acyclic piping with several separate cycles.

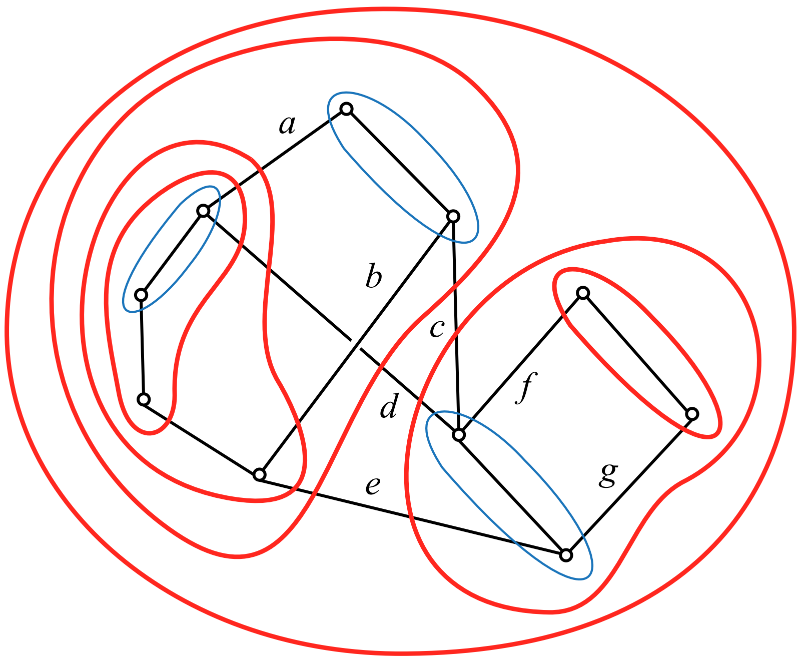

Figure 14: A maximal acyclic piping of a poset with 4 independent cycles. These can be chosen so that $\{a, b\}$, $\{c, d\}$, $\{d, e\}$, and $\{f, g\}$ are the pairs of edges in each independent cycle such that the pair is either both outside or both inside all pipes. Choosing one edge from each pair to delete gives a spanning tree. Adding tubes to make a maximal tubing of the line graph can be done so as to put the resulting points in each of the chambers of the hyperplane arrangement.

3 New realization for acyclonestohedra

Since the multiplihedron has two facets that are copies of the associahedron, one for all red tubes and one for all blue tubes, we can realize the acyclic poset associahedra by using the inequalities just for one of these, the cycle equalities, and an equality for the entire facet. For the all blue facet, that would be just the lower facet inequalities, with equality for the universal blue tube, $\sum_{x_i} = 3^{n-1}$ for n edges in the poset.

Table3 shows the realization for the acyclic poset associahedron shown in Figure 5. The image of this realization is pictured in Figure 15.

4 Quotients of the multiplihedra

In the original description of the multiplihedron, Stasheff considered a simplification for the case of a function (a homotopy homeomorphism) from a homotopy associative space, to a strictly associative space.

(lower) facets		equalities
$x_a \geq 1$	$x_c + x_d \geq 3$	
$x_b \geq 1$	$x_d + x_e \geq 3$	facet equality
$x_c \geq 1$	$x_a + x_e \geq 3$	$x_a + x_b + x_c + x_d + x_e = 81$
$x_d \geq 1$	$x_a + x_b + x_c \geq 9$	
$x_e \geq 1$	$x_c + x_d + x_e \geq 9$	cycle equality
$x_a + x_b \geq 3$	$x_a + x_d + x_e \geq 9$	$x_a - x_b + x_c - x_d + x_e = 0$
$x_b + x_c \geq 3$	$x_a + x_b + x_e \geq 9$	

Table 3: The realization for the fishy poset acyclic associahedron, using variables $(x_a, x_b, x_c, x_d, x_e)$ with subscripts from the edges of the diagram in Figure 5. An image of the realization is in Figure 15.

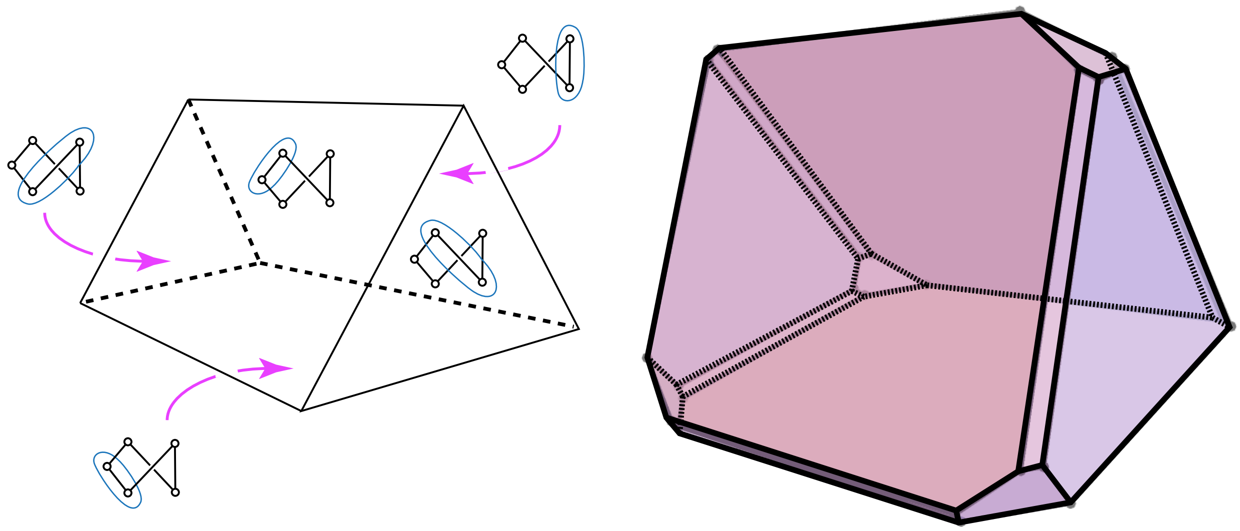

Figure 15: On the left is the order polytope $O(P)$ for the poset from Figure 5. On the right is an image of our new realization for the acyclonestohedron.

The multiplihedron in this case collapses to become the associahedron. The corresponding equivalence for colored tubings is generated by equating tubings which only differ by the addition of one red tube. For the graph multiplihedron it has been shown that these equivalence classes yield the polytope known as the graph cubeahedron, with faces also described by design tubings.

In enriched category theory the alternative quotient was also seen to be important: the case in which the homotopy homomorphism has an associative domain and homotopy associative codomain. This corresponds to equivalence for colored tubings generated by equating tubings which only differ by the addition of one blue tube. These *graph composihedra* are described in [13] as the domain quotients of graph multiplihedra.

Finally, the equivalence relation generated by both kinds of tube addition, for graph multiplihedra, is seen to give the Boolean lattice, and more importantly, the face poset of the hypercubes.

Here we define the acyclic poset cubeahedra and acyclic poset composihedra as the posets resulting from equivalence relations on the acyclic poset multiplihedra generated by addition of red and blue pipes respectively.

Definition 2. Given a poset P define the acyclic composihedron $\mathcal{J}_d(P)$ to be the poset of equivalence classes of acyclic pipings of the Hasse diagram, under the equivalence relation generated by addition of an acyclic blue pipe to a given piping. Define the acyclic design associahedron, or cubeahedron, $\mathcal{J}_r(P)$ to be the poset of equivalence classes of acyclic pipings of the Hasse diagram, under the equivalence relation generated by addition of a red acyclic pipe to a given piping.

Taken together, the equivalence on maximal pipings (vertices of the acyclic multiplihedron) under both sorts of addition is seen to give a lattice that could be termed the acyclic poset version of the Boolean lattice, or the *acyclic Boolean lattice*. However, we show here that it is already correctly described as the lattice of faces of the order polytope. More importantly, on all pipings, the equivalence under both sorts of addition of tubes is conjectured to give the face lattice of a new polytope that is actually recognizable. It is in fact the interval polytope of the face lattice of the order polytope of the poset. We can show a clear poset bijection, but the realization as a polytope is more difficult at first look.

Theorem 2. *For a poset P the equivalence classes of colored pipings under additions of red or blue pipes form a poset that is isomorphic to the poset of intervals in the face lattice of the order polytope of P.*

Proof. We describe the bijection f which takes an interval A of acyclic partitions, in the face lattice of the order polytope $\mathcal{O}(P)$, to an equivalence class $f(A)$ of the colored pipings.

Given a collection A of connected acyclic partitions of the nodes of P, where $A = [X, Y]$ is an interval in the face lattice of $\mathcal{O}(P)$, we create a colored piping from A by:

1. Discard the singleton parts in any member of A; that is ignore them for the purpose of defining the following tubes;

2. For the minimal member X of A, any non-singleton part of X which is broken into smaller parts in the remainder of the interval becomes a purple tube of $f(A)$.

3. For the minimal member X of A, any non-singleton part of X which is not broken into smaller parts in the remainder of the interval becomes a blue tube of $f(A)$.

4. For the maximal member Y of A, any non-singleton part of Y becomes a blue tube of $f(A)$.

5. If the minimal member X of A is not the minimal element of the lattice of $\mathcal{O}(P)$ (the trivial partition) then the universal tube of $f(A)$ is red.

The construction of $f(A)$ is seen to give a minimal representative of the equivalence class of colored tubings, from which no red or blue tubes can be removed without changing that class. The vertices of the interval lattice (faces of the order polytope lattice) are taken to vertices of the quotient lattice of tubings. Also, the ordering relation of the intervals is preserved by our map, since containment of sub intervals becomes resolving purple tubes (when red, the resolved tube is then dropped to reflect the equivalence under addition of red inside of red), or addition of blue tubes inside of purple (when added outside a blue tube, the inner tube is dropped to reflect the equivalence under addition of blue inside of blue). □

Examples of the mapping from the proof of Theorem 2 can be seen in Figures 19 and 20. The latter figure shows the vertex labels of both polytopes for the diamond poset, in corresponding location. Then any face shown in Figure 19 can be compared with the corresponding face in the right-hand polytope of Figure 20. The face labels of the interval polytope are simply $[X, Y]$ where X and Y are the minimal and maximal vertices of that face, that is, the minimal and maximal elements of an interval in the face lattice of the order polytope.

When the poset P is acyclic, with a Hasse diagram that is a tree, then the order polytope $\mathcal{O}(P)$ is a simplex. The acyclic Boolean lattice is the Boolean lattice, and the interval polytope of the order polytope is the hypercube. This situation recaptures a special case of quotients of the graph multiplihedron (of the line graph of the Hasse diagram of P) as described in the general case in [13].

By using the realization of the acyclic poset multiplihedron, there is an obvious way to achieve realizations of the quotients. However it is not just by performing the quotient on the graph multiplihedron and then finding a cross section of that quotient polytope. That is due to the fact that the quotient on the graph multiplihedron is under additions of red and blue tubes regardless of acyclicity. Note for instance that the corresponding cross section of the hypercube does not yield the trapezohedron (the trapezohedron is the correct result for the diamond poset). Rather it is required to follow the other order, first simplify the new realization of the acyclic multiplihedron and then take the quotient. Thus the realizations for these quotients need a dedicated proof, so we conjecture here and leave that proof for future work.

Conjecture 1. *Given equivalence relations on colored pipings of a poset P, generated by 1) addition of blue pipes, 2) addition of red pipes, and 3) generated by both additions; the resulting posets are realized as polytopes found by collapsing faces of the acyclic multiplihedron. In the third case, with both equivalences, the result is the interval polytope of the order polytope of P.*

To realize each quotient, experimentally it appears to give the correct result if we remove from the realization of the full acyclic poset multiplihedron the facet inequalities which correspond to facets now equivalent to lower dimensional faces by addition of a single red or blue acyclic tube. At the same time the remaining facet inequalities must be extended, with their constant set equal to the max power of 3 for single red tubes, or equal to 1 for single blue tubes.

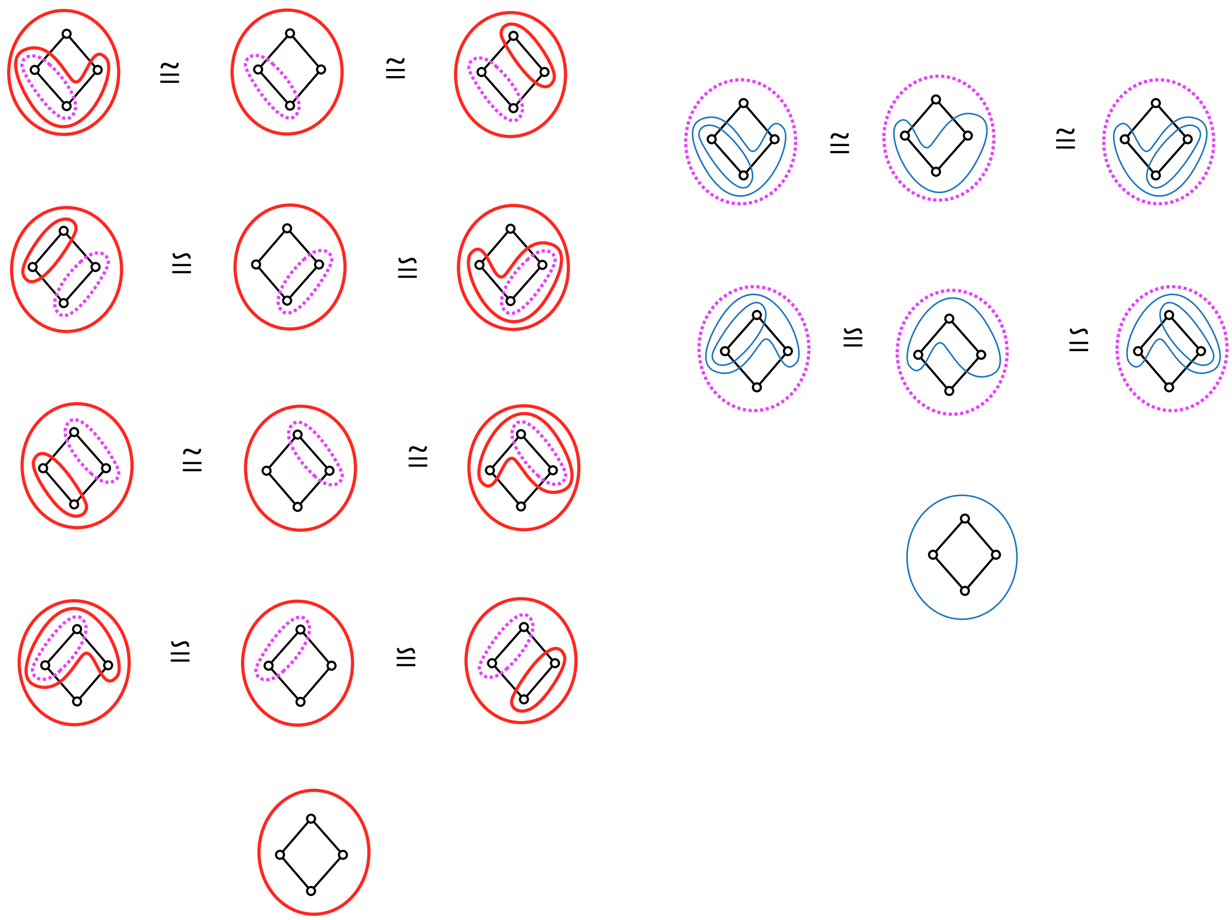

Figure 16: Facet pipings (center of each column of equivalences) of the diamond poset, corresponding to facet inequalities to be dropped from the realization to achieve (left column) the acyclic design associahedron (cubeahedron) and (right column) the acyclic composihedron. Equivalences are shown for the facets that become lower dimensional faces, under addition of red or blue tubes.

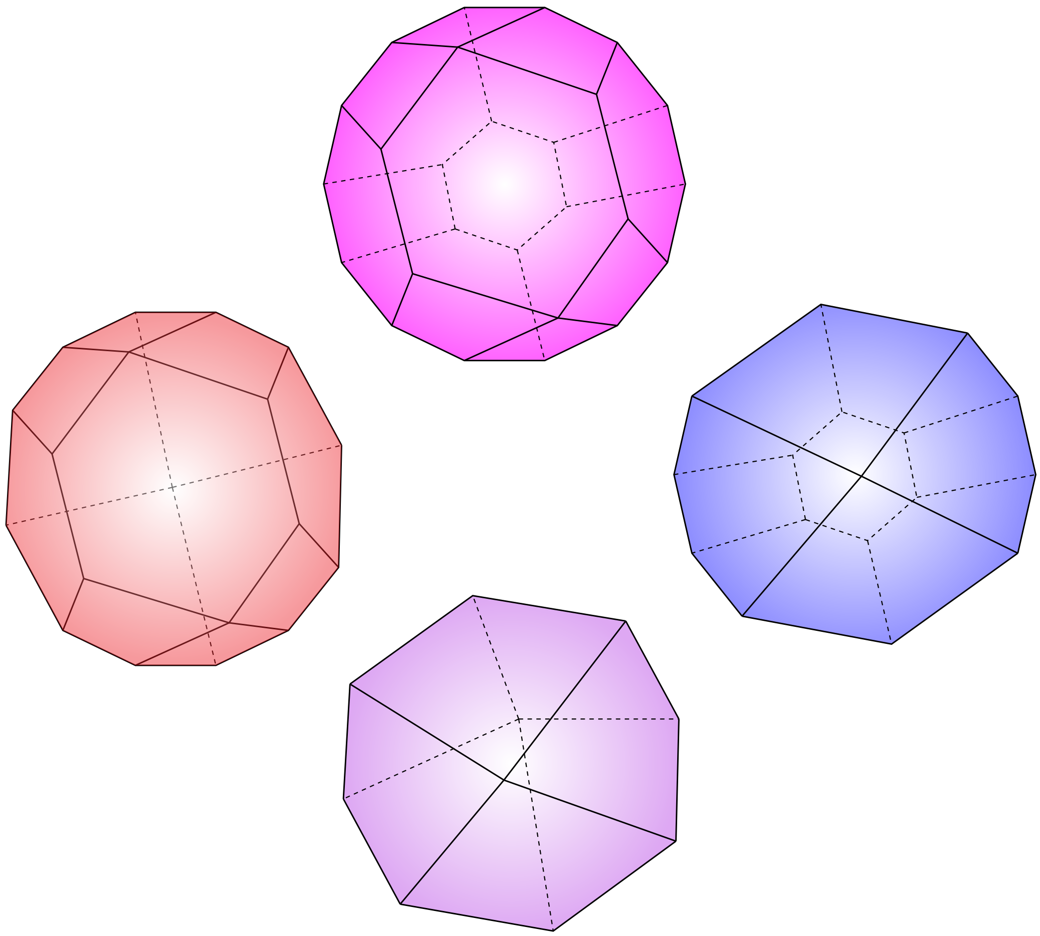

Figure 17: Top: the multiplihedron for the acyclonestohedron of the four-element diamond poset. On the left is the domain quotient, on the right the range quotient, and at the bottom is the interval polytope of the order polytope of the diamond. Note that this interval polytope of the order polytope is a trapezohedron, with a side view in Figure 19. It turns out to be the same polytope as for the bowtie poset, as seen in Figure 1.

Table 4, first column, shows the realization for the acyclic cubeahedron (range quotient, under addition of red tubes), or acyclic design associahedron, of the diamond poset. Compare to Table 1, where five upper facets have been removed corresponding to the first column of Figure 16, and the remaining four upper facets have had their constant maximized accordingly. The acyclic design associahedron (cubeahedron) has f-vector (17, 26, 11) as seen on the right of Figure 17.

acyclic cubeahedron	acyclic composihedron	order interval polytope
$x_a \geq 1$	$x_a + x_b \leq 72$	$x_a + x_b \leq 81$
$x_b \geq 1$	$x_c + x_d \leq 72$	$x_c + x_d \leq 81$
$x_c \geq 1$	$x_a + x_d \leq 75$	$x_a + x_d \leq 81$
$x_d \geq 1$	$x_b + x_c \leq 75$	$x_b + x_c \leq 81$
$x_a + x_b \geq 3$	$x_a + x_b + x_c \leq 78$	$x_a \geq 1$
$x_c + x_d \geq 3$	$x_b + x_c + x_d \leq 78$	$x_b \geq 1$
$x_a + x_b + x_c + x_d \geq 27$	$x_a + x_b + x_d \leq 78$	$x_c \geq 1$
$x_a + x_b \leq 81$	$x_a + x_c + x_d \leq 78$	$x_d \geq 1$
$x_c + x_d \leq 81$	$x_a + x_b + x_c + x_d \leq 81$	
$x_a + x_d \leq 81$	$x_a \geq 1$	
$x_b + x_c \leq 81$	$x_b \geq 1$	
	$x_c \geq 1$	
	$x_d \geq 1$	
cycle equality		
$x_a - x_b + x_c - x_d = 0$	$x_a - x_b + x_c - x_d = 0$	$x_a - x_b + x_c - x_d = 0$

Table 4: The realizations for the diamond poset acyclic cubeahedron, composihedron, and interval polytope using variables (x_a, x_b, x_c, x_d) with subscripts from the edges of the diagram in Figure 8. Compare to Table 1, where certain facets have been removed or maximized according to the equivalences in Figure 16. An image of all the polytopes is in Figure 17, and the realizations are pictured in Figure 18.

Table 4, second column, shows the realization for the acyclic composihedron, or domain quotient (under addition of blue tubes), of the diamond poset. Compare to Table 1, where three lower facets have been removed according to the first column of Figure 16. The only lower facets remaining already had their constant minimized. The acyclic composihedron has f-vector (19, 30, 13) as seen on the left of Figure 17.

Table 4, third column, shows the realization for the acyclic interval polytope, the simultaneous domain and range quotient for the diamond poset, using variables (x_a, x_b, x_c, x_d) with subscripts from the edges of the diagram in Figure 8. The acyclic interval polytope has f-vector (10, 16, 8) as seen on the bottom of Figure 17.

Acknowledgments

Thanks to Andrew Sack and to Vincent Pilaud for helpful conversations and encouragement.

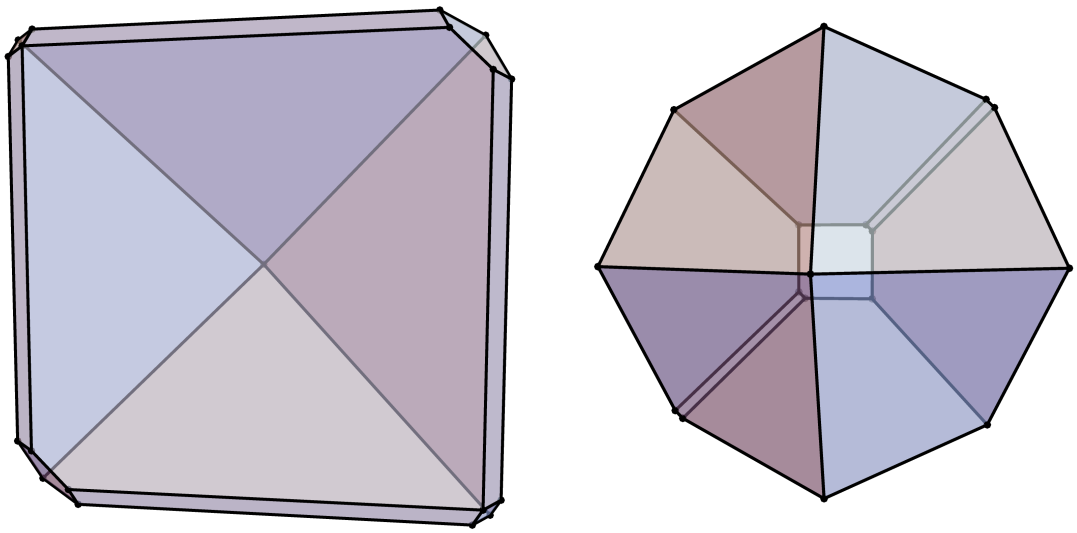

Figure 18: Results of the realization of the acyclic composihedron and cubeahedron (acyclic design associahedron) for the diamond poset, as given in Table 4.

References

[1] Federico Ardila and Jeffrey Doker. Lifted generalized permutahedra and composition polynomials. *Adv. in Appl. Math.*, 50(4):607–633, 2013.

[2] Federico Ardila-Mantilla, Nima Arkani-Hamed, Carolina Figueiredo, and Francisco Vazão. Combinatorics of the cosmohedron, 2026.

[3] Nima Arkani-Hamed, Carolina Figueiredo, and Francisco Vazão. Cosmohedra, December 2024.

[4] Spencer Backman, Nathaniel Bottman, and Daria Poliakova. Higher-categorical associahedra, 2024.

[5] Jose Bastidas, Félix Gélinas, Vincent Pilaud, Germain Poullot, Andrew Sack, and Eleni Tzanaki. Interval hypergraphic polytopes (or deformed associahedra), tamari interval posets, and weeping willows, 2026.

[6] Carolina Benedetti, Nantel Bergeron, and John Machacek. Hypergraphic polytopes: combinatorial properties and antipode. *J. Comb.*, 10(3):515–544, 2019.

[7] Nantel Bergeron and Vincent Pilaud. Interval hypergraphic lattices. *European J. Combin.*, 132(part B):Paper No. 104285, 33, 2026.

[8] Nathaniel Bottman. 2-associahedra. *Algebr. Geom. Topol.*, 19(2):743–806, 2019.

[9] Nathaniel Bottman and Daria Poliakova. Constrainahedra, 2022.

[10] Michael Carr and Satyan Linus Devadoss. Coxeter complexes and graph-associahedra. *Topology and its Applications*, 153(12):2155–2168, 2006.

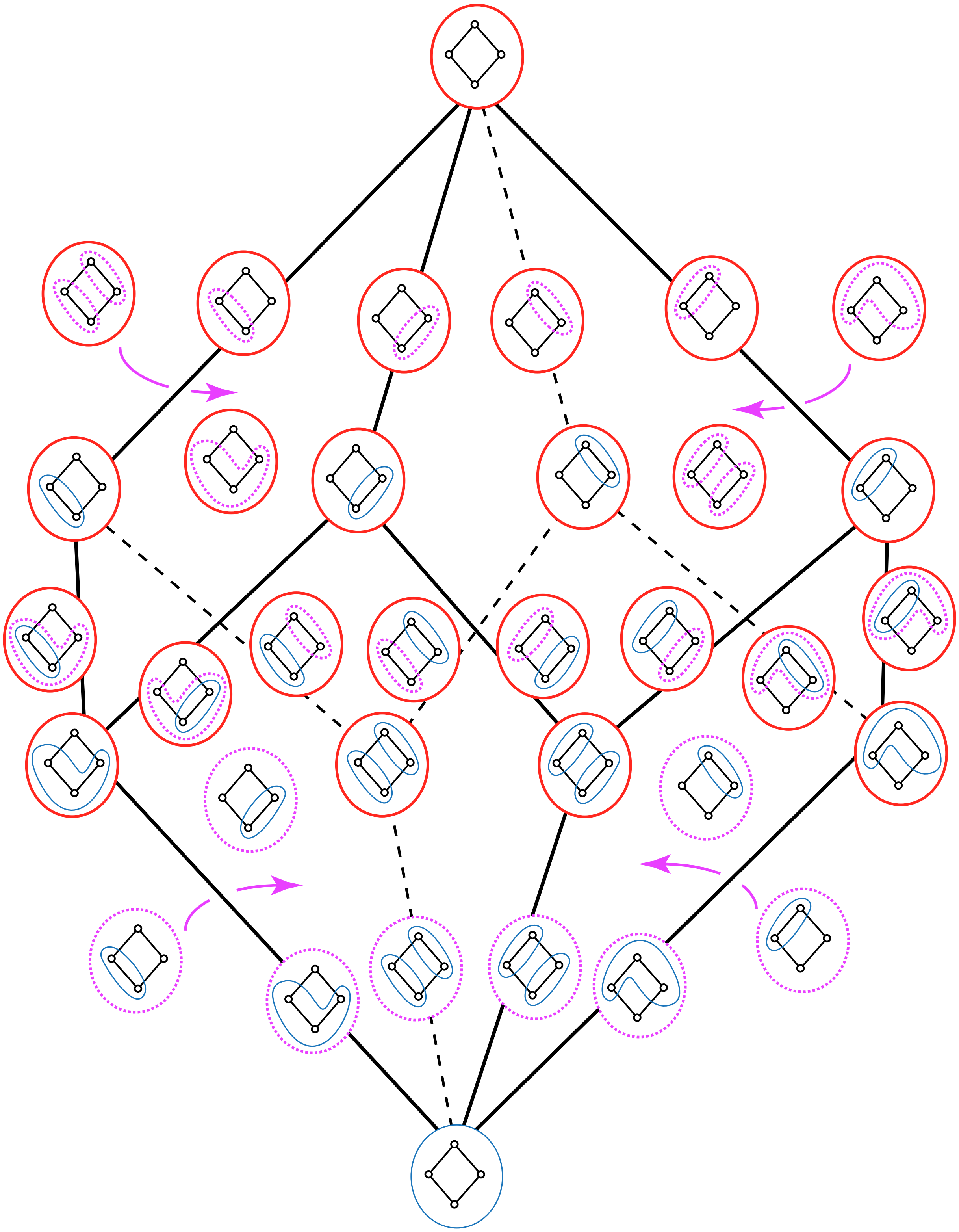

Figure 19: All face labels of the quotient of the diamond poset acyclic multiplihedron, under both equivalences.

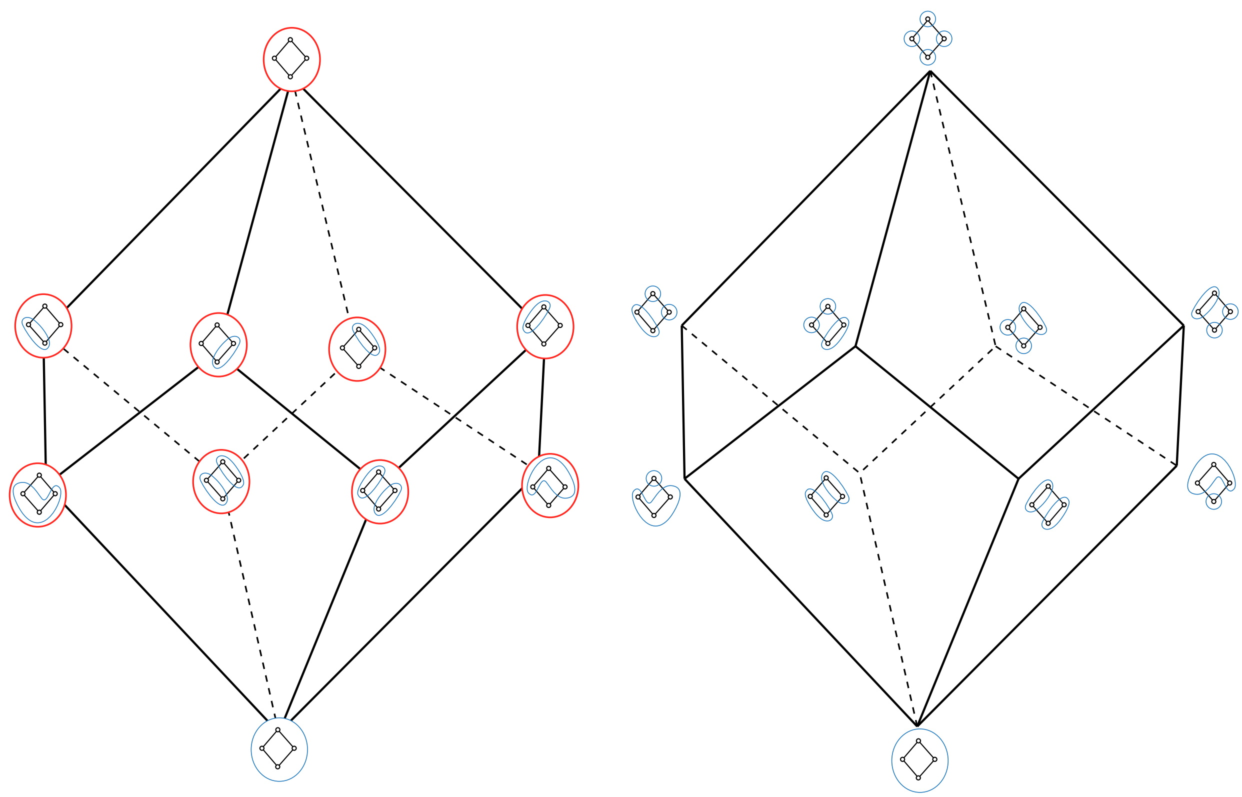

Figure 20: Vertex labels of the quotient of the diamond poset acyclic multiplihedron, under both equivalences: seen in bijection with the vertex labels of the interval polytope of the order polytope of the same poset. These vertices are the faces of the order polytope, as seen in Figure 4.

[11] Frédéric Chapoton and Vincent Pilaud. Shuffles of deformed permutahedra, multiplihedra, constrainahedra, and biassociahedra. *Ann. H. Lebesgue*, 7:1535–1601, 2024.

[12] Colin Defant and Andrew Sack. Operahedron lattices, February 2024.

[13] Satyan Devadoss and Stefan Forcey. Marked tubes and the graph multiplihedron. *Algebr. Geom. Topol.*, 8(4):2081–2108, 2008.

[14] Satyan Linus Devadoss, Stefan Forcey, Stephen Reisdorf, and Patrick Showers. Convex polytopes from nested posets. *European Journal of Combinatorics*, 43:229–248, January 2015.

[15] Stefan Forcey. Convex hull realizations of the multiplihedra. *Topology Appl.*, 156(2):326–347, 2008.

[16] Stefan Forcey, Ross Glew, and Hyungrok Kim. Generalised wavefunction coefficients and acyclonestocosmohedra. *J. Phys. A*, 58(46):Paper No. 465403, 27, 2025.

[17] Pavel Galashin (Павел Галашин). P-associahedra. *Selecta Mathematica, New Series*, 30(1):6, 2024.

[18] Ross Glew and Tomasz Łukowski. Amplitubes: Graph cosmohedra. *Journal of High Energy Physics*, 2025.

[19] Guillaume Laplante-Anfossi. The diagonal of the operahedra. *Advances in Mathematics*, 405:108494, August 2022.

[20] Chiara Mantovani, Arnau Padrol, and Vincent Pilaud. Acyclonestohedra. *Séminaire Lotharingien de Combinatoire*, 91B:28, April 2024.

[21] Chiara Mantovani, Arnau Padrol, and Vincent Pilaud. Facial nested complexes and acyclonestohedra, 2025.

[22] Vincent Pilaud and Francisco Santos. Multitriangulations as complexes of star polygons. *Discrete Comput. Geom.*, 41(2):284–317, 2009.

[23] Vincent Pilaud and Francisco Santos. Quotientopes. *Bull. Lond. Math. Soc.*, 51(3):406–420, 2019.

[24] Alexander Evgenievich Postnikov (Александр Евгеньевич Постников). Permutohedra, associahedra, and beyond. *International Mathematics Research Notices*, 2009(6):1026–1106, 2009.

[25] Andrew Sack. A realization of poset associahedra. *Séminaire Lotharingien de Combinatoire*, 89B:24, April 2023.

[26] James Dillon Stasheff. Homotopy associativity of H-spaces. I, II. *Trans. Amer. Math. Soc.*, 108:293–312, 1963. 108 (1963), 275-292; ibid.